

56-07
N88-15806 118081
308

ADVANCED PROPELLER RESEARCH

John F. Groeneweg
and
Lawrence J. Bober

ABSTRACT

Recent results of aerodynamic and acoustic research on both single and counter-rotation propellers are reviewed. Data and analytical results are presented for three propellers: SR-7A, the single rotation design used in the NASA Propfan Test Assessment (PTA) flight program; CRP-X1, the initial 5+5 Hamilton Standard counter-rotating design; and F7-A7, the 8+8 counterrotating General Electric design used in the proof-of-concept Unducted Fan (UDF) engine. In addition to propeller efficiencies, cruise and takeoff noise, and blade pressure data, off-design phenomena involving formation of leading edge vortices are described. Aerodynamic and acoustic computational results derived from three-dimensional Euler and acoustic radiation codes are presented. Research on unsteady flows, which are particularly important for understanding counterrotation interaction noise, unsteady loading effects on acoustics, and flutter or forced response is described. The first results of three-dimensional unsteady Euler solutions are illustrated for a single rotation propeller at angle of attack and for a counter-rotation propeller. Basic experimental and theoretical results from studies of the unsteady aerodynamics of oscillating cascades are outlined. Finally, advanced concepts involving swirl recovery vanes and ultra bypass ducted propellers are discussed.

OUTLINE

The material in this presentation addresses three aspects of propeller research, analysis, verification of the analysis with experiment, and studies of advanced concepts, and is covered in four major divisions. Single rotation and counter-rotation technology address cruise performance, noise at both cruise and takeoff, and other topics including blade pressure measurements, flow phenomena associated with off-design operation, and steady Euler analyses. In the area of unsteady aerodynamics, recent unsteady three-dimensional Euler results are shown along with theoretical and experimental results from work on transonic cascades. Finally, advanced concepts and the future work to address them are discussed.

OUTLINE

- **SINGLE ROTATION TECHNOLOGY**
- **COUNTERROTATION TECHNOLOGY: GEARED & GEARLESS**
- **UNSTEADY AERODYNAMICS**
- **ADVANCED CONCEPTS—FUTURE WORK**

CD-87-29480

ADVANCED PROPELLER DESIGN PARAMETERS

Recent wind tunnel tests have provided data on these models of advanced high-speed propellers. The SR-7 is the most recent of a series of single rotation designs and is a scale model of the propeller being used in the Propfan Test Assessment (PTA) Flight Program. The F7-A7 is a scale model of the counterrotation pusher propeller being used on the unducted fan (UDF) demonstrator engine. The CRP-X1 model simulates a counterrotation tractor propeller. The nominal diameter of all these models is 2 ft.

ADVANCED PROPELLER DESIGN PARAMETERS

	NUMBER OF BLADES	RADIUS RATIO	CRUISE MACH NUMBER	CRUISE LOADING, shp/D ²	TIP SPEED, ft/sec
SR-7	8	0.24	0.80	32.0	800
F7-A7	8+8	0.425	0.72	55.5	780
CRP-X1	5+5	0.240 0.275	0.72	37.2	750

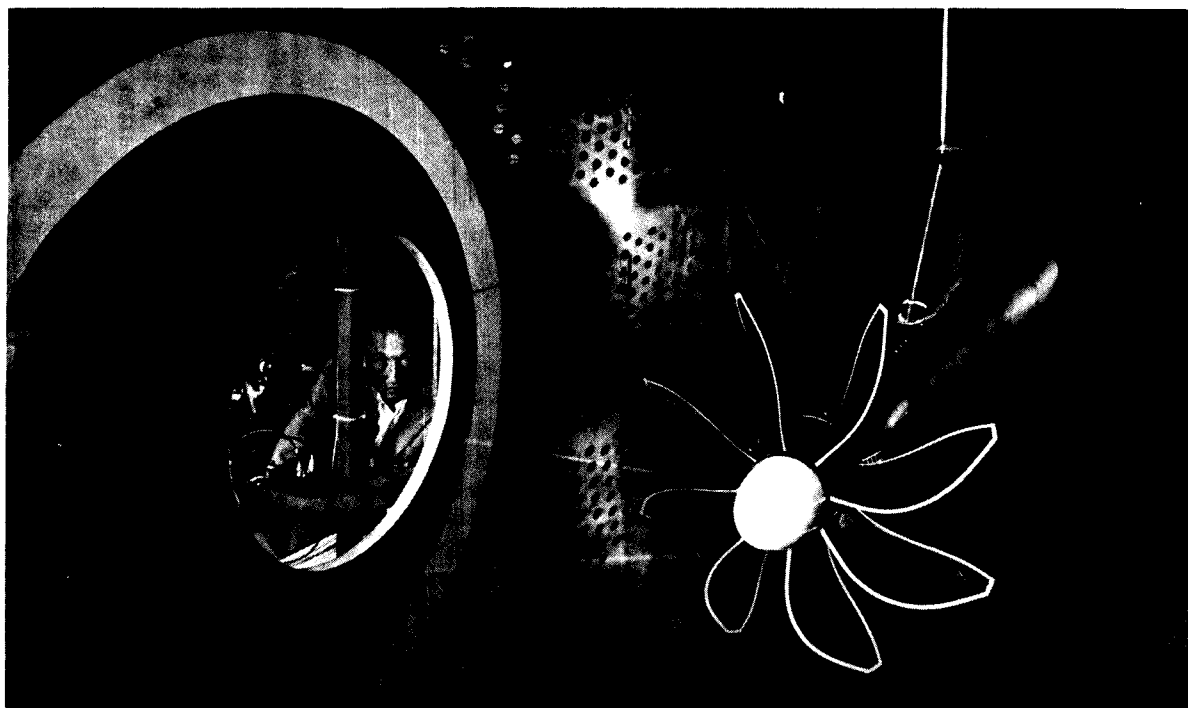
CD-87-29481

ORIGINAL PAGE IS
OF POOR QUALITY

SR-7A PROPELLER IN LEWIS 8- BY 6-FT WIND TUNNEL

The propeller model, SR-7A, is an aeroelastically scaled model of the LAP propeller (SR-7L) which is being used in the PTA flight program. The model is shown in the NASA Lewis 8- by 6-foot wind tunnel, where it was tested for aerodynamic, acoustic, and aeroelastic performance. Also shown in the photograph are laser beams which were part of a system for measuring blade deflections during propeller operation.

SR-7A PROPELLER IN LEWIS 8- BY 6- FT WIND TUNNEL



CD-87-29482

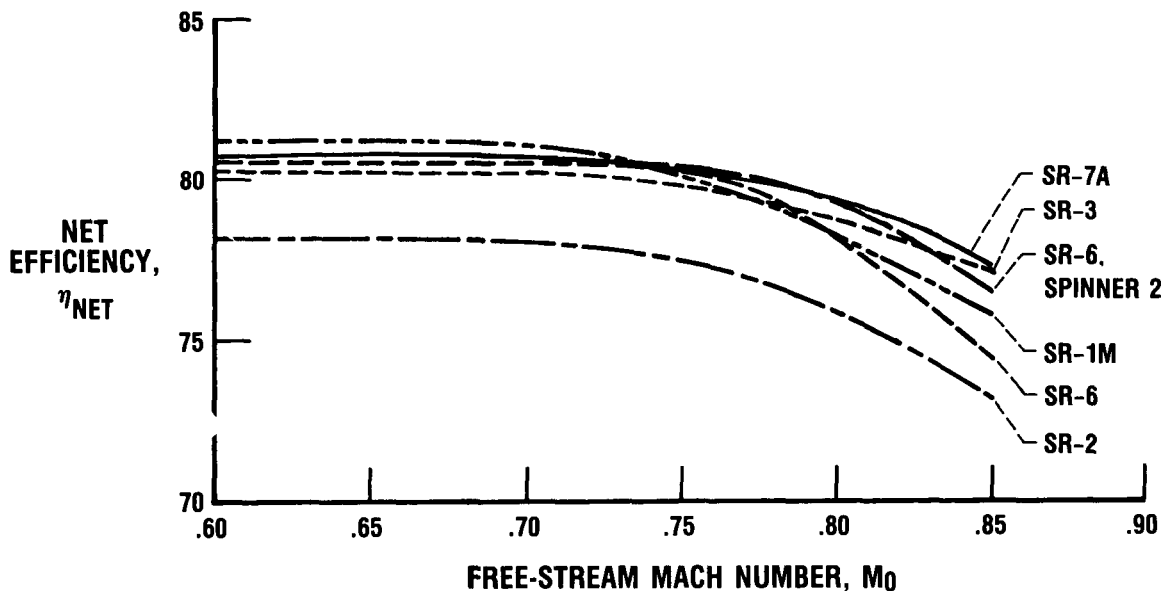
SINGLE-ROTATION PROPELLER PERFORMANCE

Net efficiency of the SR-7 propeller model is shown along with results from five earlier models. The measured net efficiencies are shown as a function of Mach number with each propeller's design loading parameter C_p/J_3 kept constant with Mach number. At Mach 0.80 the SR-7A propfan has the highest measured propeller efficiency of 79.3 percent. The performance of the SR-2 propeller is lower than the performance of the other propellers since it is the only one of these models which has no blade sweep. Important characteristics of these models are indicated below.

Design	Number of blades	Sweep angle, deg	Power coefficient, C_p	Advance ratio, J	Loading parameter, C_p/J_3
SR-7A	8	41	1.45	3.06	0.0509
SR-6	10	40	2.03	3.50	.0474
^a SR-6	10	40	2.03	3.50	.0474
SR-3	8	45	1.70	3.06	.0593
SR-1M	8	30	1.70	3.06	.0593
SR-2	8	0	1.70	3.06	.0593

^aEstimated performance with alternate spinner 2.

SINGLE-ROTATION PROPELLER PERFORMANCE

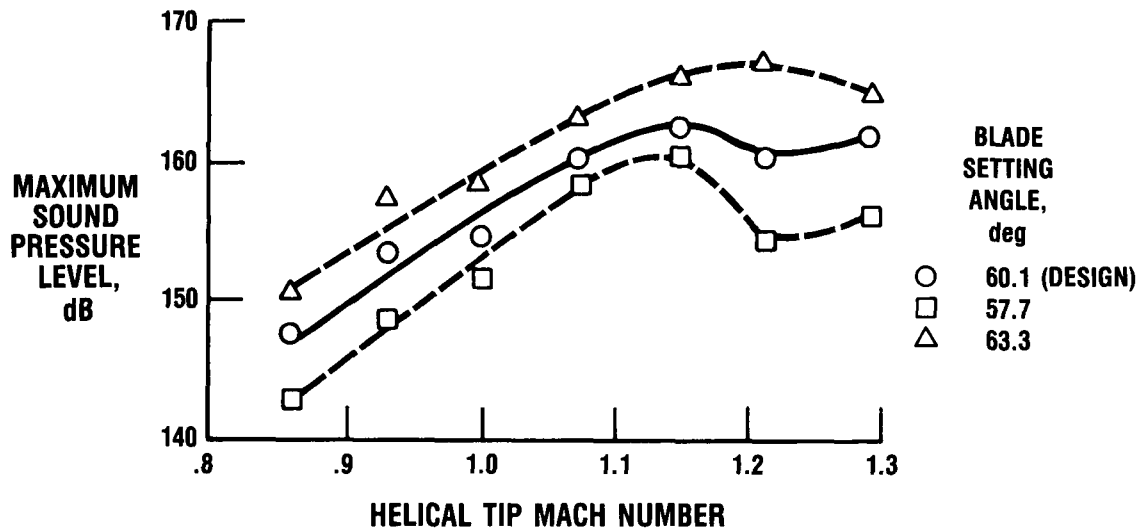


CD-87-29483

SR-7 PEAK BLADE PASSING TONE VARIATION WITH HELICAL TIP MACH NUMBER

Peak fundamental tone levels are shown at constant advance ratio (3.06) for three loading levels as indicated by the blade setting angles bracketing the design value. The striking feature of the tone variation with helical tip Mach number is the behavior in the supersonic range beyond 1.1. The peak fundamental tone levels no longer increase and may peak, level off, or decrease depending on loading. This result indicates that higher cruise and propeller speeds do not necessarily mean increased cabin noise problems.

SR-7 PEAK BLADE PASSING TONE VARIATION WITH HELICAL TIP MACH NUMBER CONSTANT ADVANCE RATIO, 3.06

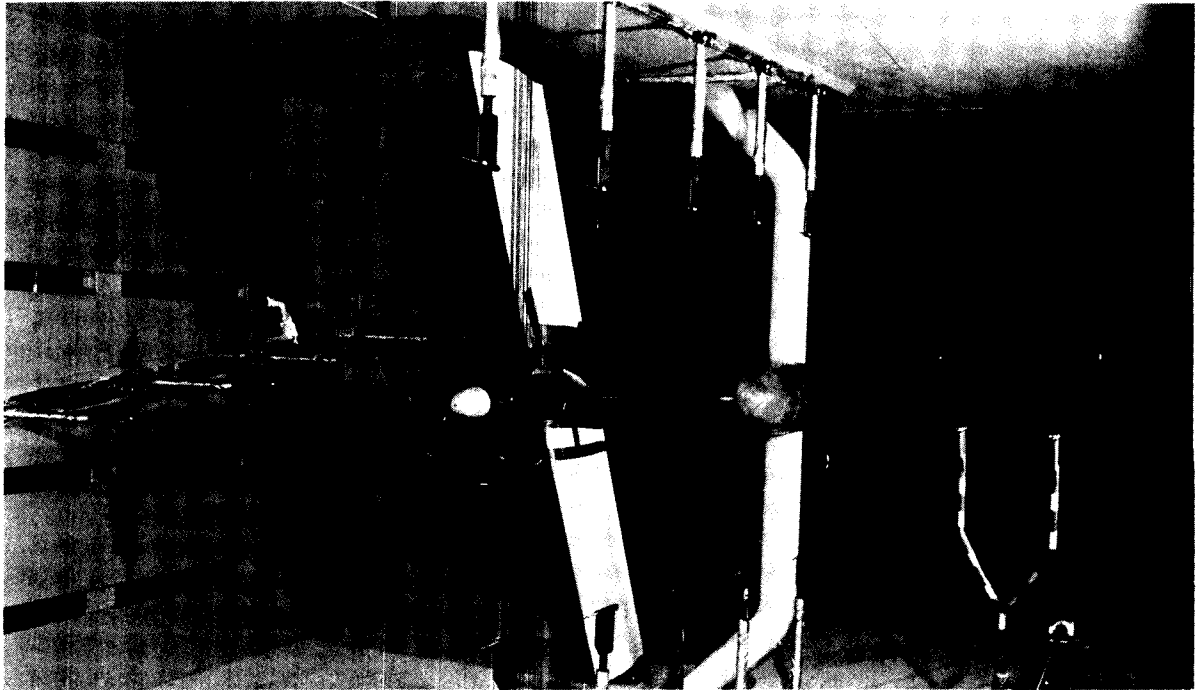


CD-87-29484

SR-7A PROPELLER MODEL IN THE 9- BY 15-FT ANECHOIC WIND TUNNEL

The SR-7A propeller model is shown installed on a swept wing used to determine installation effects on community noise at typical takeoff and approach conditions (Mach 0.2). The entire propeller-wing assembly may be rotated to angle of attack in the horizontal plane. The continuously traversing microphones (at right) measure far-field noise corresponding to levels measured below an aircraft during flyover. Fixed microphones on the walls measure noise in the other three directions and are staggered with respect to the tunnel flow to avoid wake interference on downstream microphones. The walls are acoustically treated to provide anechoic conditions down to a frequency of 250 Hz, well below the fundamental frequency for the propeller model.

SR-7A PROPELLER MODEL IN 9- BY 15-FT ANECHOIC WIND TUNNEL



CD-87-29485

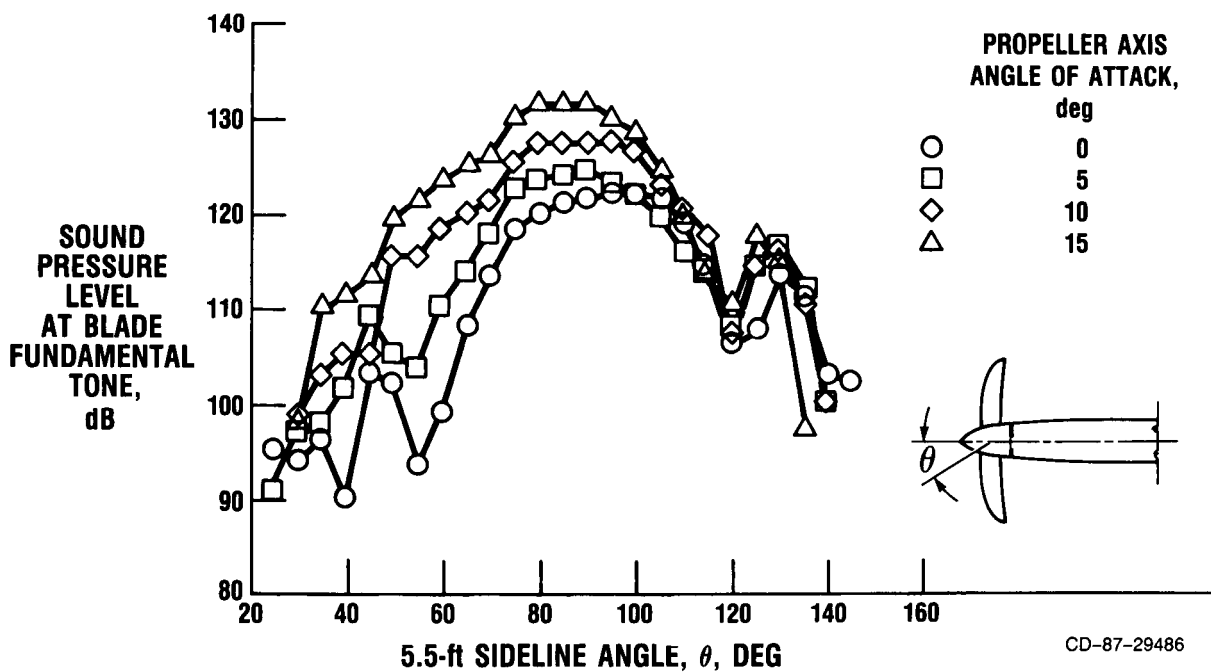
ORIGINAL PAGE IS
OF POOR QUALITY

EFFECT OF ANGLE OF ATTACK ON FLYOVER NOISE

Fundamental tone directivities are shown for four angles of attack ranging from 0 to 15°. The peak levels, approximately in the plane of rotation, increased by about 10 dB. A typical maximum takeoff angle of the propeller centerline with respect to the aircraft flight path is about 8°; thus takeoff noise would be increased of the order of 5 dB due to unsteady loading at that angle of attack.

EFFECT OF ANGLE OF ATTACK ON FLYOVER NOISE

SINGLE-ROTATION PROPELLER SR-7A; 9- BY 15-ft WIND TUNNEL; TAKEOFF BLADE ANGLE, 37.8°; TIP SPEED, 800 ft/sec; TUNNEL MACH NUMBER, 0.2

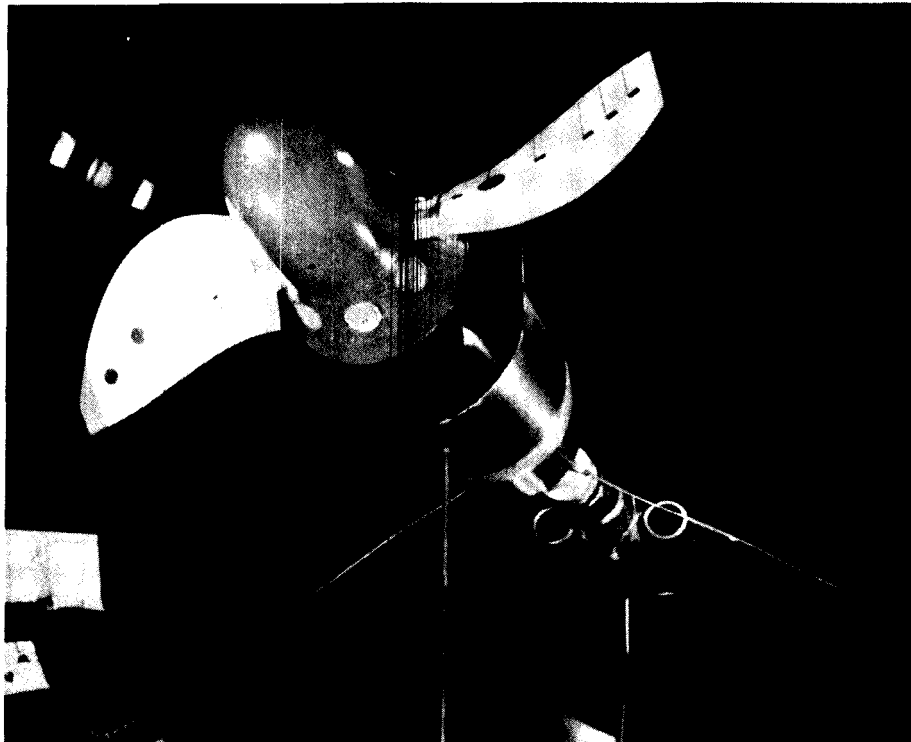


ORIGINAL PAGE IS
OF POOR QUALITY

TWO-BLADE VERSION OF LARGE-SCALE ADVANCED PROPFAN (LAP)

A two-blade version of the eight-blade large-scale advanced propeller (LAP) was tested in the ONERA S1 wind tunnel to obtain steady and unsteady blade pressures over a wide range of operating conditions. Only two blades were used because of the limited total power available to drive the propeller. In this way the propeller could be operated at a reasonable power per blade. The large size of this propeller (9 ft diameter) allowed much more detailed measurements than could be obtained on the 2-ft-diameter models tested previously.

TWO-BLADE VERSION OF LARGE-SCALE ADVANCED PROPFAN (LAP)

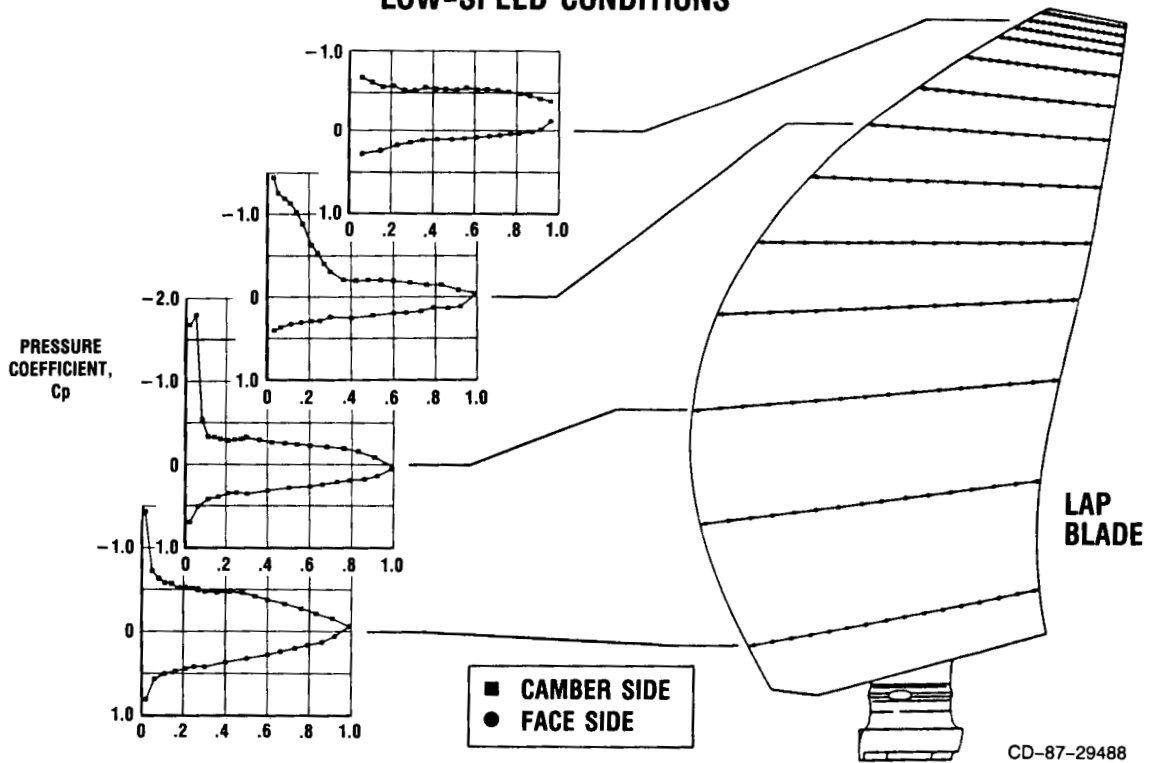


CD-87-29487

BLADE PRESSURE MEASUREMENTS ON FULL-SCALE PROPELLER

Steady blade pressure distributions are shown at several spanwise locations on the SR-7L at a low-speed, high-power condition. The pressure distributions at the two locations nearest the tip lack the high suction peaks of the inboard locations because of the presence of the leading edge and tip vortices at the outboard locations. Similar data were obtained at 12 additional operating conditions, providing valuable data for code verifications.

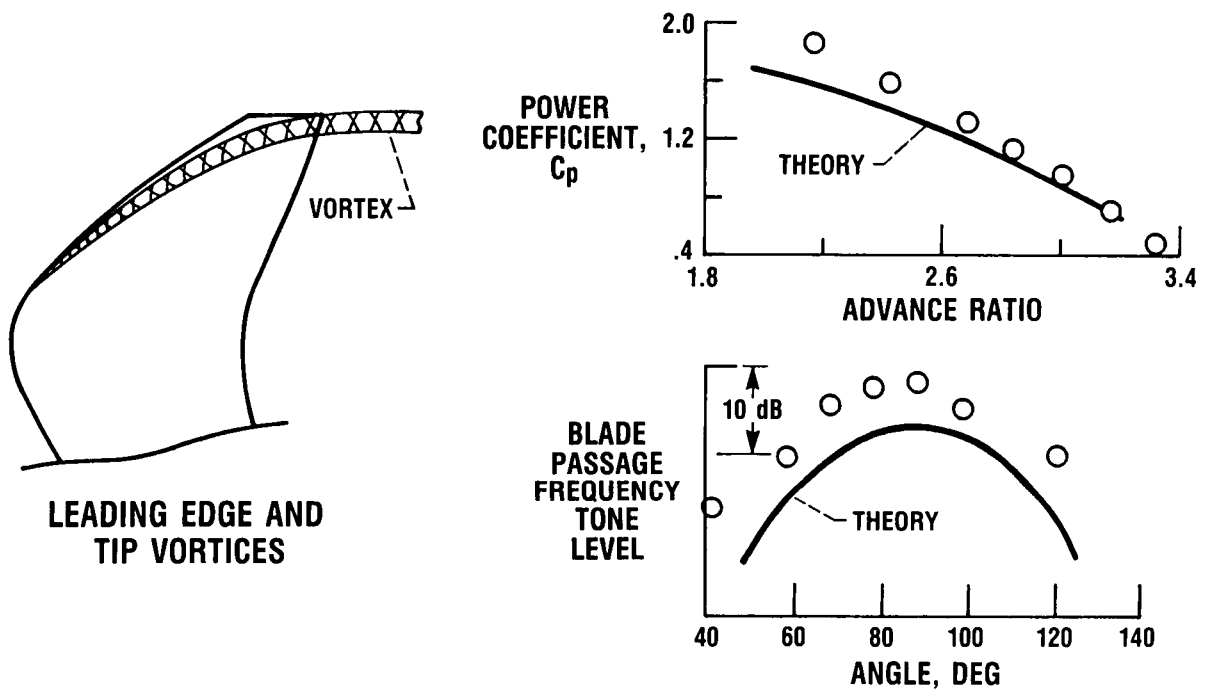
BLADE PRESSURE MEASUREMENTS ON FULL SCALE PROPELLER LOW-SPEED CONDITIONS



OFF-DESIGN PROPELLER OPERATION

When the propeller is operating appreciably off-design (cruise), such as at takeoff, a leading edge vortex which merges with the tip vortex is expected to form as shown schematically. The phenomenon is similar to the vortex structure on a delta wing aircraft at high angle of attack during approach. If the associated altered loading distribution is not accounted for in analytical models, errors in aerodynamic performance and the tone noise level predictions will result as illustrated.

OFF-DESIGN OPERATION



CD-87-29489

VISUALIZATION OF PROPELLER BLADE SURFACE FLOW
AT OFF-DESIGN CONDITIONS

The fluorescent oil flow patterns on the pressure side of the SR-3 blade at the Mach 0.8, windmill condition are shown. Streaks in the oil at the blade surface are influenced by two main factors. Centrifugal forces cause radial flow in the oil film. Shear flow forces at the surface act mainly along streamlines. Over much of the blade the streaks are at an angle determined by these two forces. However, near the leading edge on the outboard portion of the blade and at the tip, the lines are primarily radial. This indicates a different flow regime, interpreted as the existence of a leading edge vortex merging with a tip vortex.

**VISUALIZATION OF PROPELLER BLADE SURFACE FLOW
OFF-DESIGN CONDITIONS**



CD-87-29490

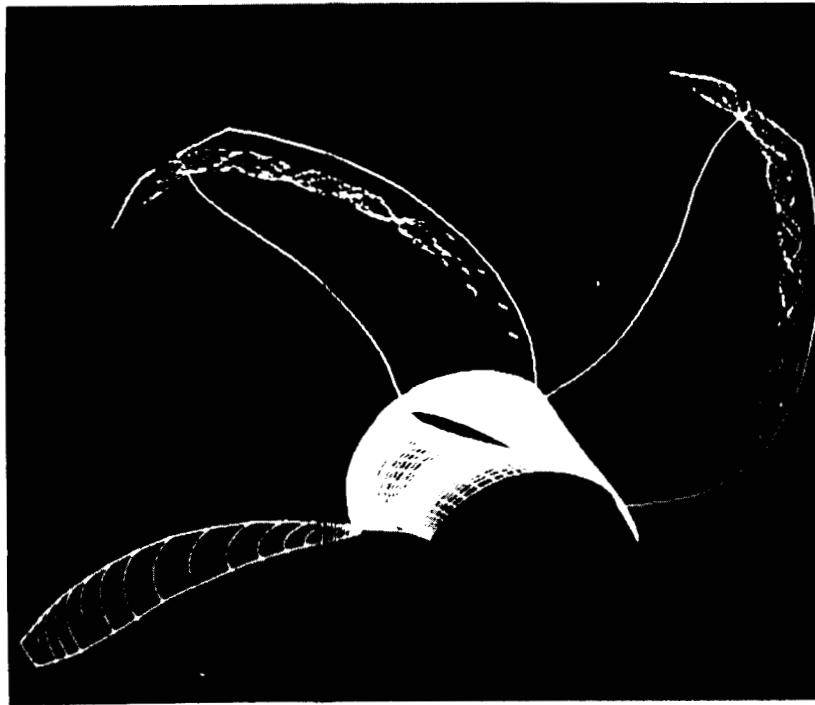
ORIGINAL PAGE IS
OF POOR QUALITY

ORIGINAL PAGE IS
OF POOR QUALITY

COMPUTED STREAMLINES ON CRP-X1 PROPELLER

An Euler code developed at Lewis was run at United Technologies Research Center (UTRC) with an order of magnitude increase in grid points to about 200 000. When particle paths were traced they revealed the leading edge vortex which merges with the tip vortex flow. The operating condition at Mach 0.2 and advance ratio of 1.0 is typical of a takeoff situation which involves high incidence angles. Apparently, numerical "viscosity" is sufficient to trigger vortex formation and produce at least a qualitative description of this flow phenomenon.

COMPUTED STREAMLINES ON CRP-X1 PROPELLER MACH 0.2; J = 1.0



CD-87-29491

COUNTERROTATING PROPELLER (CRP-X1) IN UTRC WIND TUNNEL

This propeller model, designated CRP-X1, was designed and built by Hamilton Standard and is shown installed in the UTRC high-speed wind tunnel. The front and rear propellers are independently driven by two air-driven turbines. Propeller performance and flow field data, as well as blade stresses were measured during these tests. Propeller acoustic data were obtained during separate tests in the UTRC Acoustic Research Tunnel.

COUNTERROTATING PROPELLER (CRP-X1) IN UTRC WIND TUNNEL



CD-87-29492

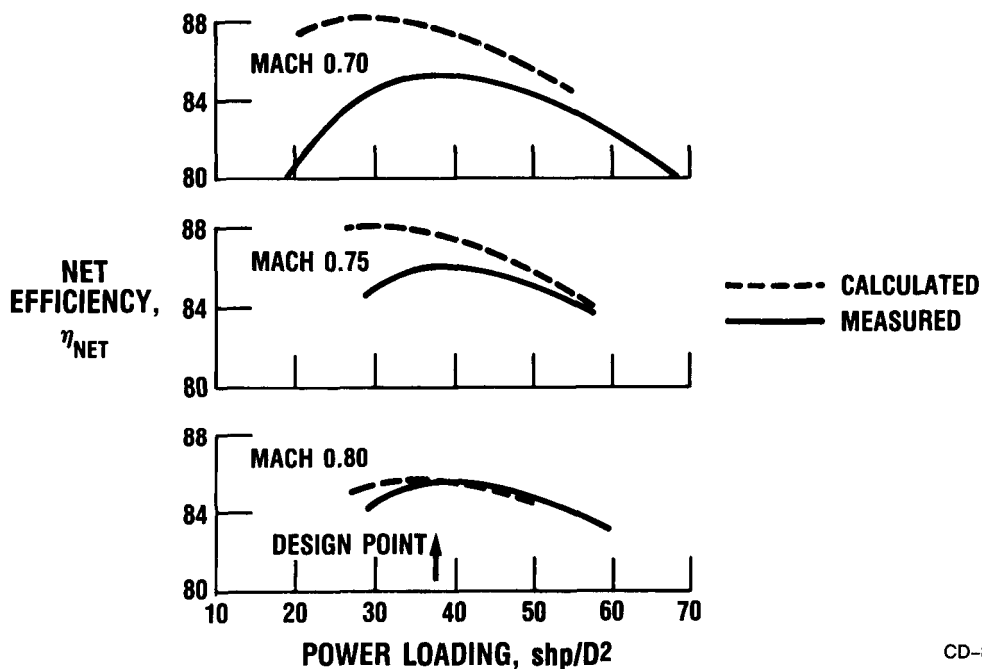
ORIGINAL PAGE IS
OF POOR QUALITY

CRP-X1 PERFORMANCE COMPARISON

The net efficiency of the CRP-X1 propeller model is shown as a function of power loading at three free-stream Mach numbers. At the design power loading of 37.2 shp/D², the data indicate a net efficiency of approximately 85 percent for Mach numbers in the range of 0.7 to 0.8. The efficiency also remains high over a wide range of power loadings. The predicted efficiency agrees very well with the data at Mach 0.8, but somewhat overpredicts the efficiency at the lower Mach numbers.

CRP-X1 PERFORMANCE COMPARISON

$\Delta\beta = 2.6^\circ$; tip speed, 750 ft/sec



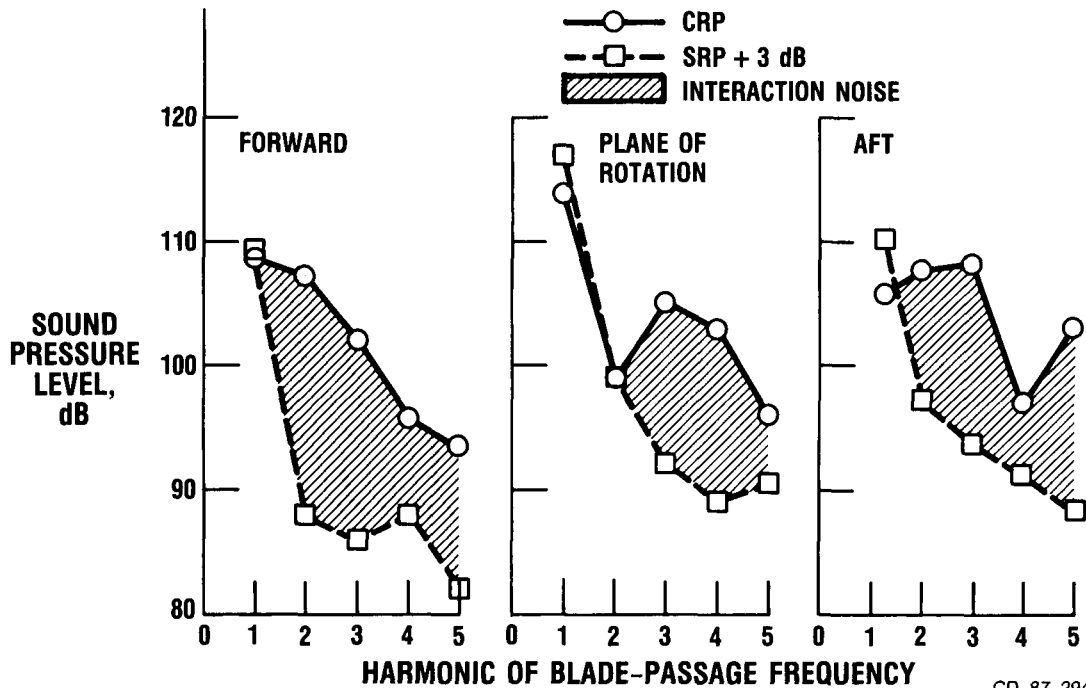
CD-87-29493

COUNTERROTATION PROPELLER INTERACTION NOISE

Levels of the first five harmonics of single-rotation (SRP) and counterrotation (CRP) propeller noise are shown at three axial locations in the far field: forward, aft, and in the plane of rotation. The single rotation fundamental tone levels are adjusted upward three decibels to compare the equivalent of two independent propellers with the CRP-X1 counterrotation configuration. Single and counterrotation fundamental tones are then roughly equal, but the counterrotation harmonic levels are dramatically higher at all locations due to the unsteady aerodynamic interactions between blade rows. This characteristic of high fore and aft harmonic levels must be dealt with to achieve acceptable counterrotation community noise levels.

COUNTERROTATION PROPELLER INTERACTION NOISE

CRP-X1 AT TAKEOFF CONDITIONS: ($V_T = 650$ ft/sec; 100 shp/rotor)

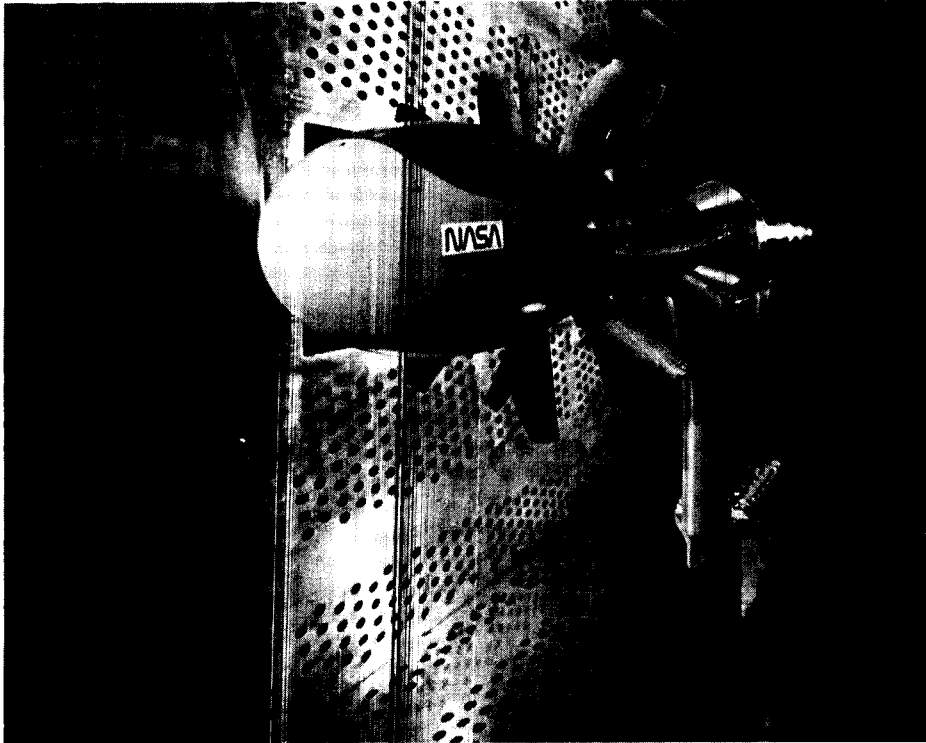


CD-87-29494

COUNTERROTATION PROPELLER IN LEWIS 8- BY 6-FT WIND TUNNEL

The NASA Lewis counterrotation pusher propeller test rig is shown installed in the 8- by 6-foot wind tunnel. The tunnel has holes in the walls equivalent to about 6 percent porosity to minimize wall interactions at transonic speeds. The rig is strut mounted and is powered by two turbines using 450-psi drive air. Performance, flow field, and acoustic measurements are made during testing.

COUNTERROTATION PROPELLER IN LEWIS 8- BY 6-FT WIND TUNNEL



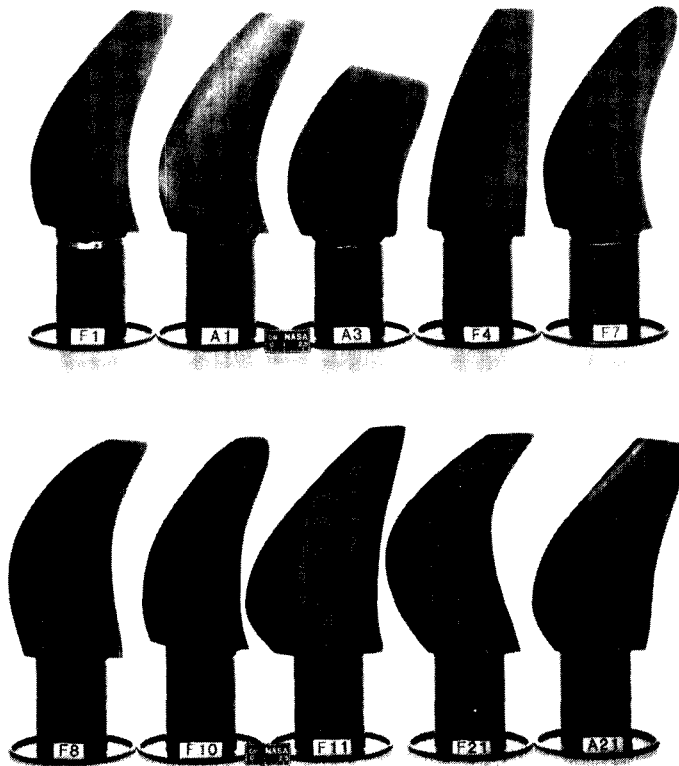
CD-87-29495

ORIGINAL PAGE IS
OF POOR QUALITY

MODEL COUNTERROTATION PROPELLER BLADES

The blade configurations tested included designs for Mach 0.72 cruise (top row) and Mach 0.8 cruise (bottom row). The designs differed in tip sweep, planform shape, airfoil camber, and a significantly shortened aft rotor (A3). The planform shapes for most forward and aft rotors were very similar. The aft rotor planform for A21 is included since it differs so much from the front rotor F21. Data from the Mach 0.72 configurations will be compared. The F1-A1 configuration is very similar to F7-A7 but with reduced camber, which is expected to improve cruise efficiency. F1-A3 was run to see the aerodynamic and acoustic effects of a short aft rotor. Both F1-A1 and F1-A3 were run with a 9+8 blade configuration as well as the standard 8+8. These blades were designed and built by the General Electric.

MODEL COUNTERROTATION PROPELLER BLADES



CD-87-29496

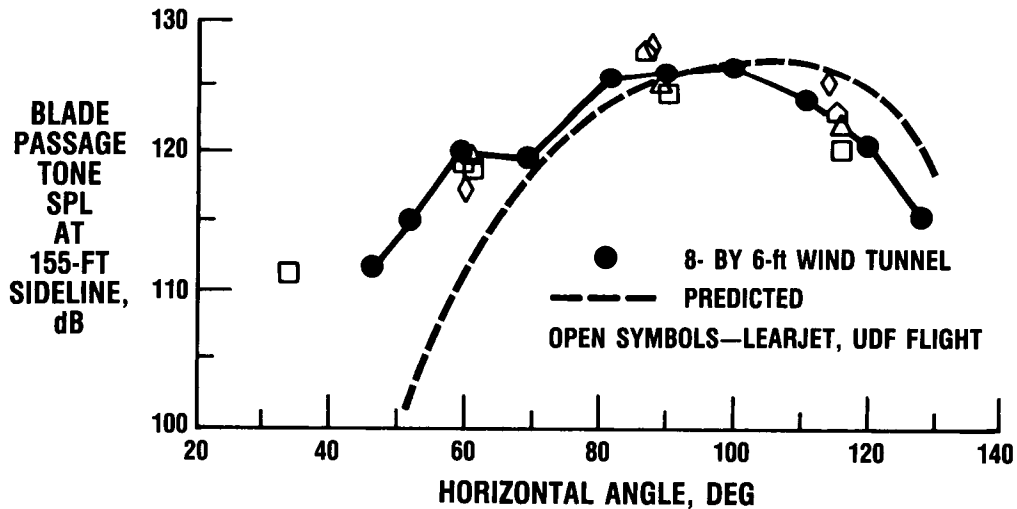
COUNTERROTATION TONE LEVELS AT CRUISE

Fundamental tone directivities for F7-A7, the proof-of-concept UDF configuration, are compared for model data from the Lewis 8- by 6-ft wind tunnel scaled to full-scale cruise conditions, full-scale flight data obtained by the formation flight of the instrumented Lewis Learjet with the UDF engine on the 727, and predicted levels from a frequency domain model developed by at General Electric. There is excellent agreement between the model wind-tunnel measurements and full-scale flight data. Predicted levels agree quite well with the data except for the forward angles. Detailed conditions for the data shown are given below:

	Forwrd/aft blade pitch, deg	Power, percent MXCL	Source
○	58.5/57.7	100	8- by 6-ft wind tunnel
□	61.6/54	100	
△	59/53.3	76	Lear jet
◇	59.3/52.9	87	
△	59.2/52.8	77	
— —	58.7/57.7	100	Predicted

COUNTERROTATION TONE LEVELS AT CRUISE

PROPELLER F7-A7; MACH 0.72; ALTITUDE, 35 000 ft

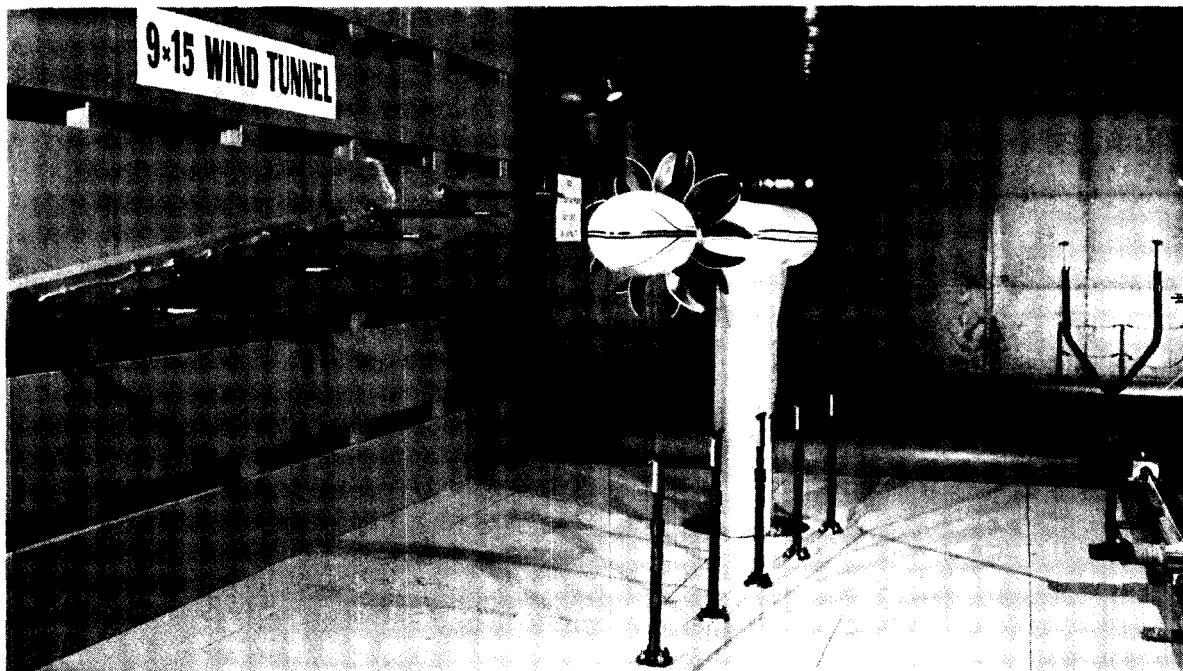


CD-87-29498

COUNTERROTATION MODEL F7-A7 IN THE LEWIS 9- BY 15-FT ANECHOIC WIND TUNNEL

The model of the 8+8 configuration of the propeller used on the UDF proof-of-concept engine is shown in the 9- by 15-ft anechoic wind tunnel where extensive community noise tests were conducted. Unequal blade numbers, differential diameter, rotor-to-rotor spacing, angle of attack, and effects of an upstream support pylon were investigated. A continuously traversing "flyover" noise microphone can be seen at right. A circumferentially traversing microphone (not shown) was also used to map the asymmetric sound field with the model at angle of attack or with a pylon installed. The tunnel walls are acoustically treated to make the test section anechoic down to 250 Hz, well below the fundamental tone frequency of the model.

COUNTERROTATION MODEL F7-A7 IN LEWIS 9- BY 15-FT ANECHOIC WIND TUNNEL



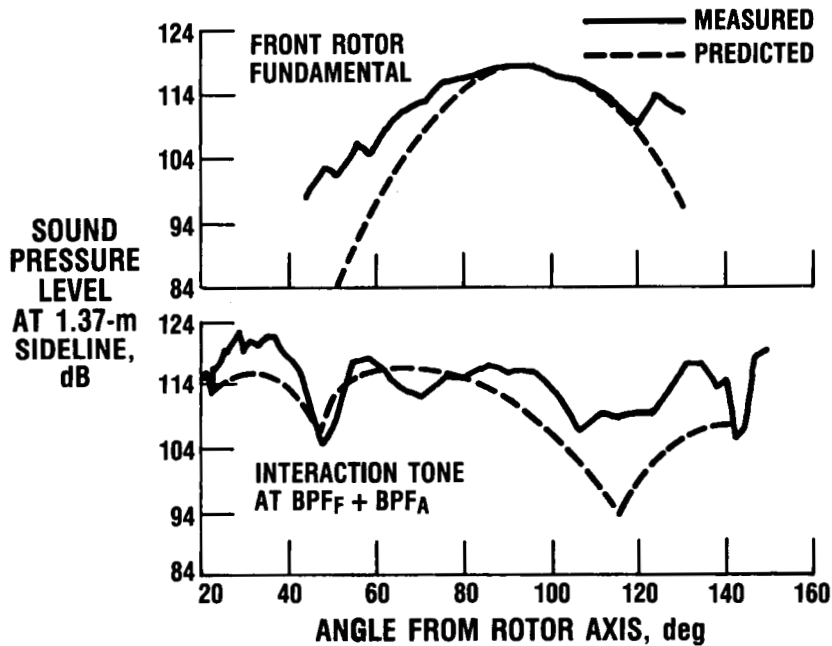
CD-87-29499

ORIGINAL PAGE IS
OF POOR QUALITY

COUNTERROTATION PROPELLER NOISE AT TAKEOFF

Measured and predicted directivities of the front rotor fundamental and the first interaction tone for F7-A7 at Mach 0.2 are compared. The predictions are from a frequency domain theory developed at General Electric. Note, again, the high levels of interaction tone noise at both forward and aft angles, in contrast to the forward rotor alone fundamental which peaks in the plane of rotation. Agreement between theory and data is very good for the front rotor fundamental. The predicted shape of the first interaction tone agrees well with the data, but the levels underpredict at the extremes in angle indicating more code development work is required for the interaction noise sources.

COUNTERROTATION PROPELLER NOISE AT TAKEOFF F7-A7; MACH 0.2; 9- BY 15-ft WIND TUNNEL

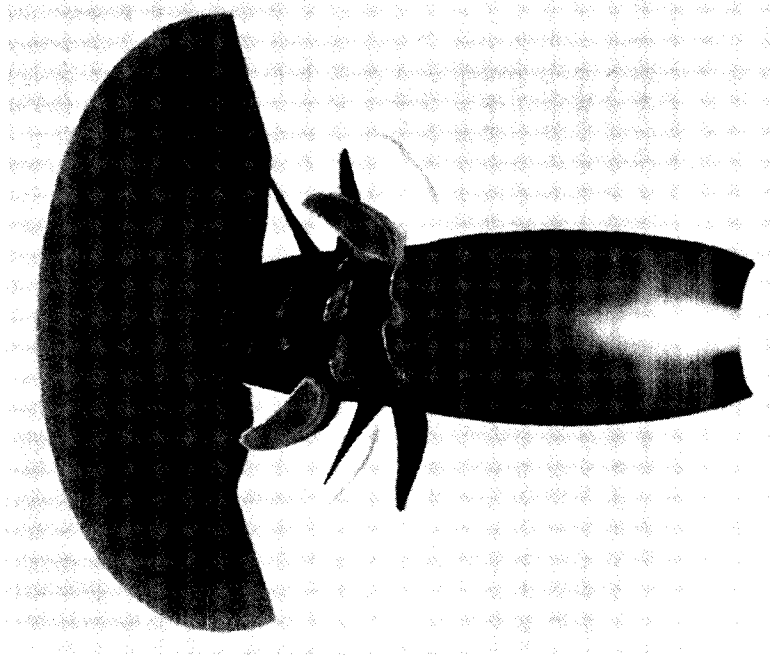


CD-87-29500

THREE-DIMENSIONAL EULER ANALYSIS OF COUNTERROTATING PROPELLER FLOW FIELD

A counterrotation Euler code developed at NASA Lewis has been used to obtain numerical predictions of the flow about one version of the General Electric UDF. The solution is obtained by iterating between the front and rear blade rows. The coupling between rows is done in an axisymmetric sense, so there are no blade-wake interactions included. This three-dimensional image shows the pressure distribution on the nacelle and blade surfaces as well as on a plane perpendicular to the axis of rotation at the aft end of the nacelle. The pressures range from high (red) to low (blue) with the yellow-green range in the middle. The flow field pressures were taken from the flow field of the rear row and show near-field acoustic pressure perturbations spiraling out into the flow. The calculations were done at Cray Research, and the flow field was displayed using the code movie-BYU.

THREE-DIMENSIONAL EULER ANALYSIS OF COUNTERROTATION PROPELLER FLOW FIELD



CD-87-29501

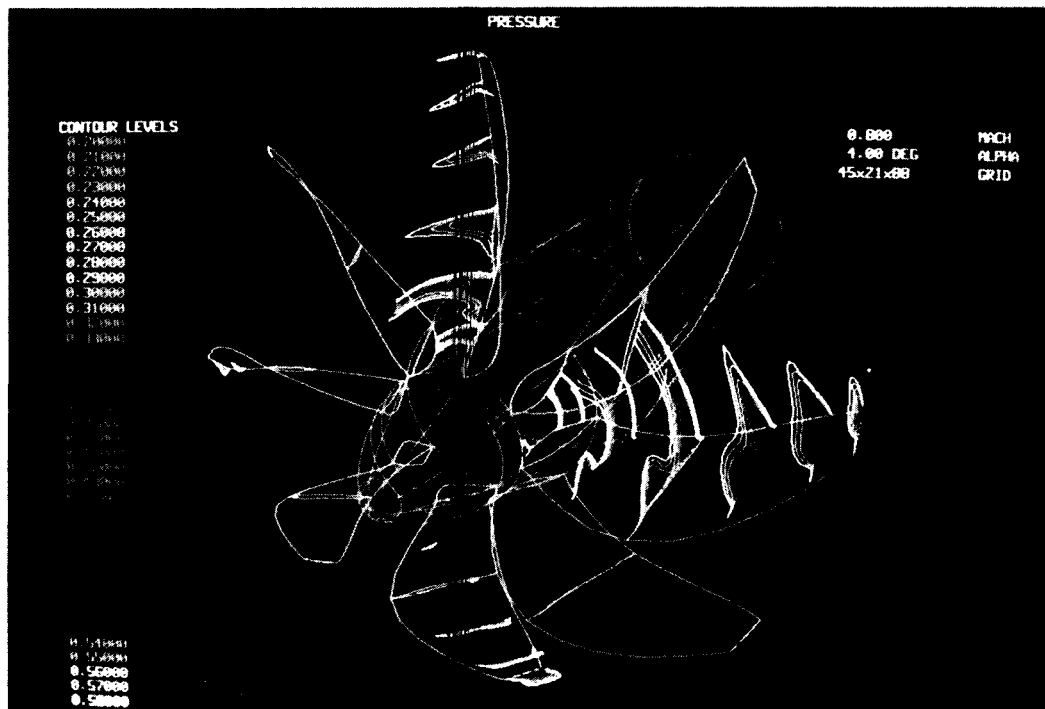
ORIGINAL PAGE IS
OF POOR QUALITY

~~REPLACES PAGE 10
OF REPORT~~

UNSTEADY THREE-DIMENSIONAL EULER CODE SOLUTION FOR PROPELLER
AT ANGLE OF ATTACK

Results from an unsteady Euler code solution for the SR-3 propeller with its axis at 4° to the mean 0.8 Mach number flow are shown. As the propeller rotates, downward moving blades (on the right in the figure) experience the highest incidence, upward blades (on the left) the lowest, and top and bottom are near the mean. Chordwise pressure distributions are plotted on the blade surfaces. Very high loadings are indicated on the blade moving downward at about 90° (on the right) where the highest incidence angles are experienced. In comparison much lower loadings are experienced by the top vertical blade, which has incidence angles near the mean value. This unsteady Euler code was developed at Mississippi State University, and graphics were done at the Air Force Arnold Engineering and Development Center.

UNSTEADY 3D EULER CODE SOLUTION FOR PROPELLER
AT ANGLE OF ATTACK



CD-87-29502

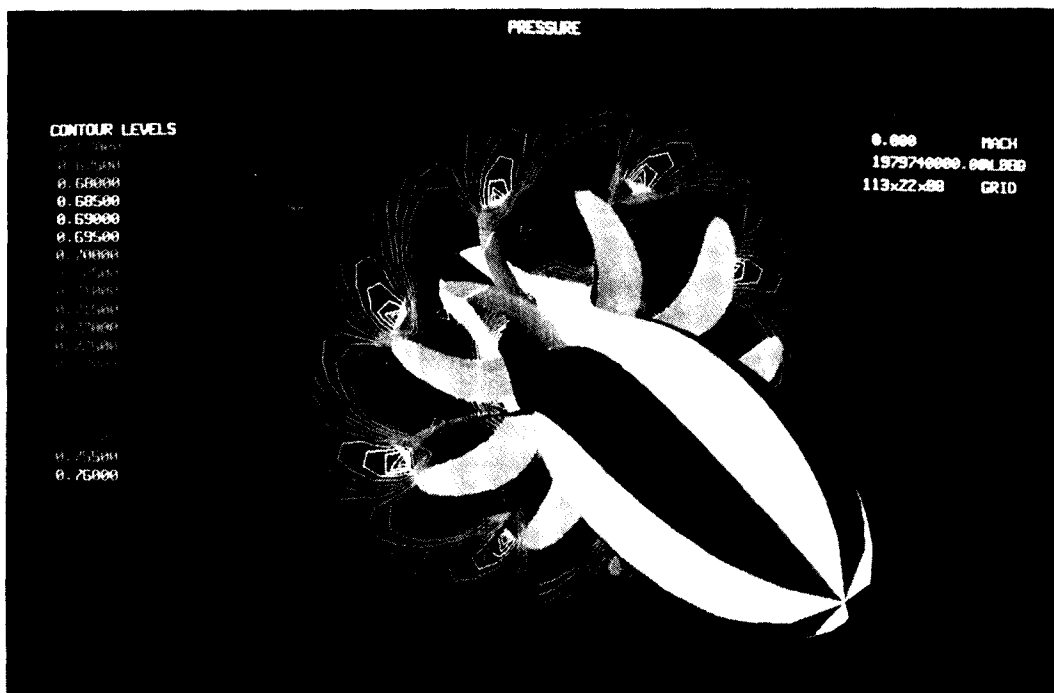
ORIGINAL PAGE IS
OF POOR QUALITY

ORIGINAL PAGE IS
OF POOR QUALITY

UNSTEADY THREE-DIMENSIONAL EULER SOLUTIONS FOR COUNTERROTATION PROPELLER

The unsteady Euler solution algorithms were also applied to the 8+8-configuration F7-A7 counterrotation propeller to obtain a full unsteady three-dimensional solution for the flow field. A sample of the results in the form of pressure contours in a plane just downstream of both blade rows is shown. These contours, which are for a particular instant in time, show an island structure indicative of the tip vortices shed by the blades. Current solution methods handle equal blade numbers in each row and are being extended to treat the general case of unequal blade numbers.

UNSTEADY 3D EULER SOLUTION FOR COUNTERROTATION PROPELLER

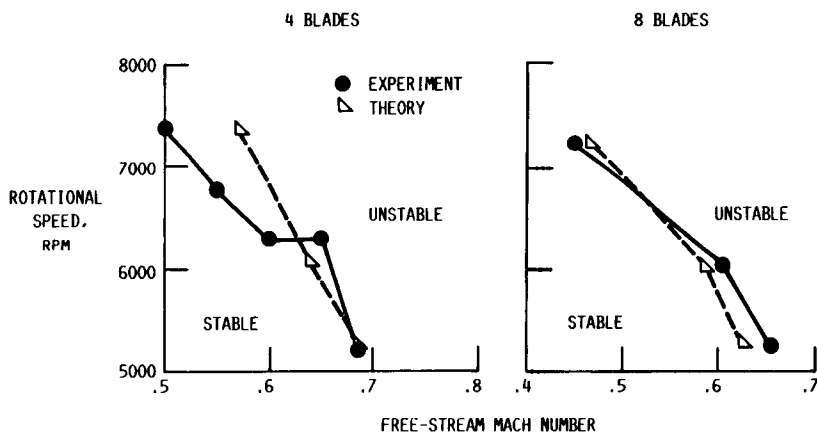


CD-87-29503

COMPARISON OF MEASURED AND CALCULATED FLUTTER BOUNDARIES

An experimental and analytical research program is being conducted to understand the flutter and forced response characteristics of advanced high-speed propellers. A comparison of measured and calculated flutter boundaries for a propfan model, called SR3C-X2, is shown in the figure. The theoretical results, from the Lewis-developed ASTROP3 analysis, include the effects of centrifugal loads and steady-state, three-dimensional air loads. The analysis does reasonably well in predicting the flutter speeds and slopes of the boundaries. However, the difference between the calculated and measured flutter Mach numbers is greater for four blades than for eight blades. This implies that the theory is overcorrecting for the decrease in the aerodynamic cascade effect with four blades.

COMPARISON OF MEASURED AND CALCULATED
FLUTTER BOUNDARIES
SR3C-X2 PROPFAN MODEL

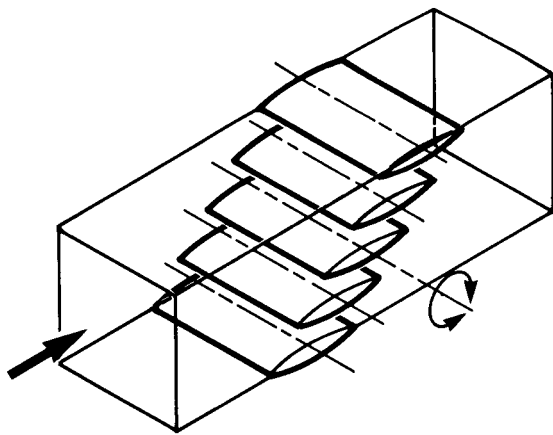


CD-87-29586

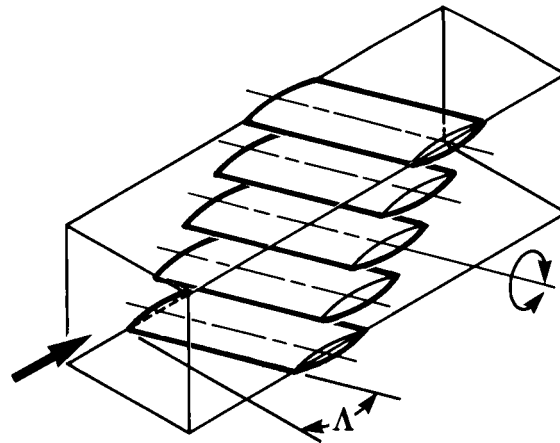
SWEPT CASCADE EXPERIMENT

Wind tunnel tests of the SR-5 propeller demonstrated that cascade effects and sweep effects have a destabilizing influence on the flutter boundary at relative Mach numbers approximately equal to one. Experimental research conducted in the NASA Lewis transonic oscillating cascade will investigate the subsonic and transonic steady and unsteady aerodynamics relevant to advanced turboprops. An unswept cascade will provide baseline data. Following that, the aerodynamics of a cascade of airfoils with sweep will be quantified. Both subsonic and transonic flow fields will be investigated as the airfoils undergo torsional oscillations at realistic reduced-frequency values.

SWEPT CASCADE EXPERIMENT



UNSWEPT CASCADE



SWEPT CASCADE

- EXPERIMENT TO DETERMINE EFFECT OF BLADE SWEEP, Λ , ON TRANSONIC CASCADE AERODYNAMICS
- STEADY AND UNSTEADY BLADE SURFACE PRESSURES
- TORSIONAL BLADE OSCILLATION
- DATA USED TO BENCHMARK STEADY AND UNSTEADY ANALYSES

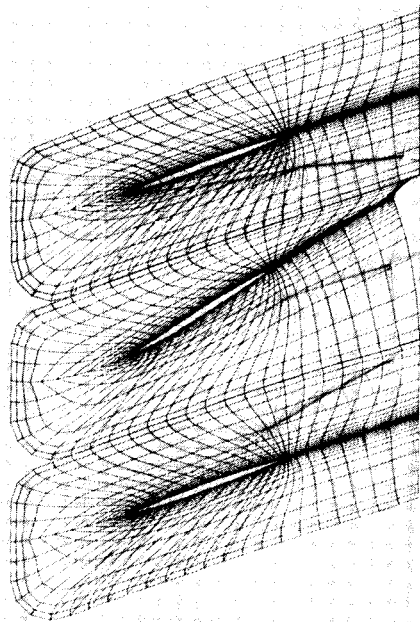
CD-87-29505

TWO-DIMENSIONAL UNSTEADY, NAVIER-STOKES
OSCILLATING CASCADE ANALYSIS

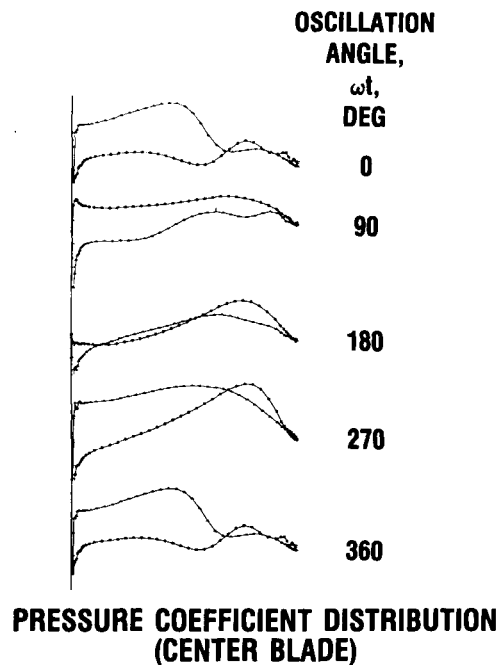
A compressible, unsteady, full Navier-Stokes, finite-difference code has been developed for modeling transonic flow through two-dimensional, oscillating cascades. The procedure introduces a deforming grid technique to capture the motion of the airfoils. The use of a deforming grid is convenient for treatment of the outer boundary conditions since the outer boundary can be fixed in space, while the inner boundary moves with the blade motion. The code is an extension of the isolated airfoil code developed at the Georgia Institute of Technology. The motion of the shock wave is evident in the chordwise pressure distributions.

2D UNSTEADY, NAVIER-STOKES, OSCILLATING CASCADE ANALYSIS

**NACA 16-004 CASCADE; $M_1 = 0.75$; $g = 1.0$; $\alpha_m = 21^\circ$; $\alpha_1 = \pm 2.0^\circ$; $k = 0.20$;
 $Re = 5.0 \times 10^6$; $\theta = 20^\circ$; $\sigma = 90^\circ$**



DEFORMING GRID (EXAGGERATED MOTION)



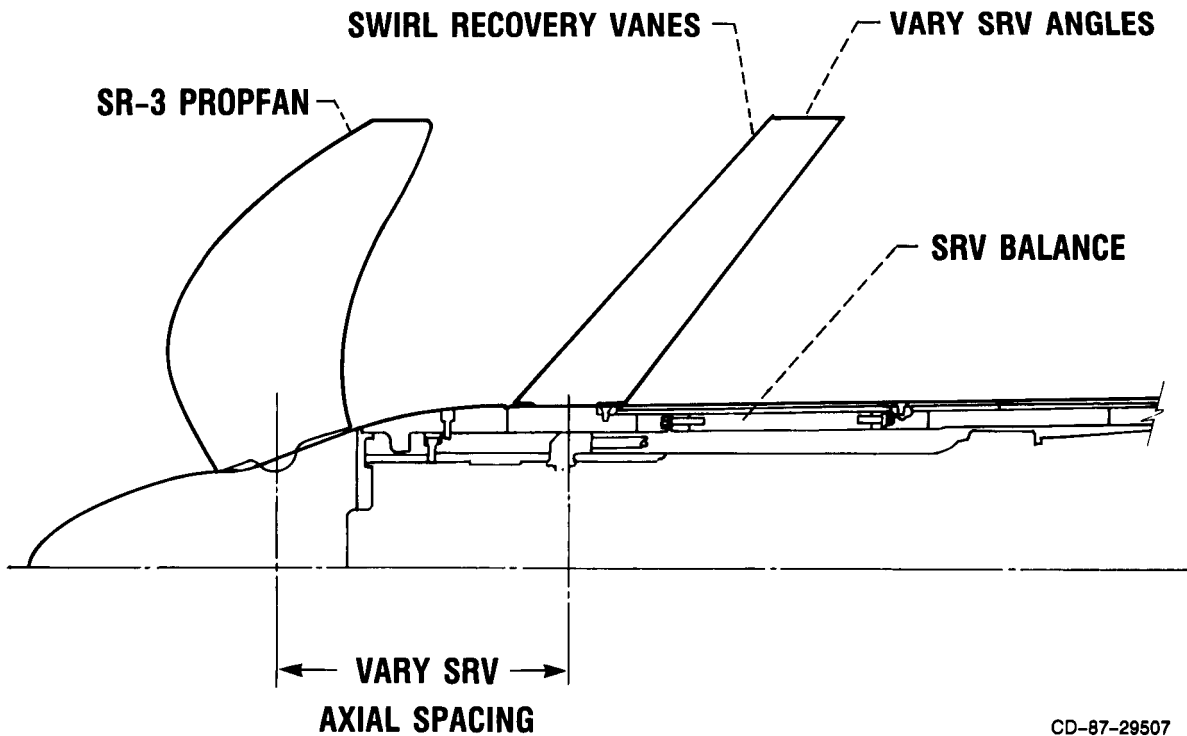
OSCILLATION ANGLE, ωt , DEG
0
90
180
270
360
PRESSURE COEFFICIENT DISTRIBUTION (CENTER BLADE)

CD-87-29506

SWIRL RECOVERY VANE EXPERIMENT

The Swirl Recover Vane Experiment will investigate the fuel saving and noise benefits available by adding swirl recovery vanes (SRV) behind a propfan. Thus, the 1000-hp single-rotation propeller test rig will be modified to accept a new balance and 12 swirl recovery vanes. These tests will determine the fuel saving benefits of the SRV concept over its Mach number operating range (0 to 0.85). Other parametric variations will include vane angle and vane axial spacing relative to the propfan. Also, flow visualization of the flow dynamics will be done.

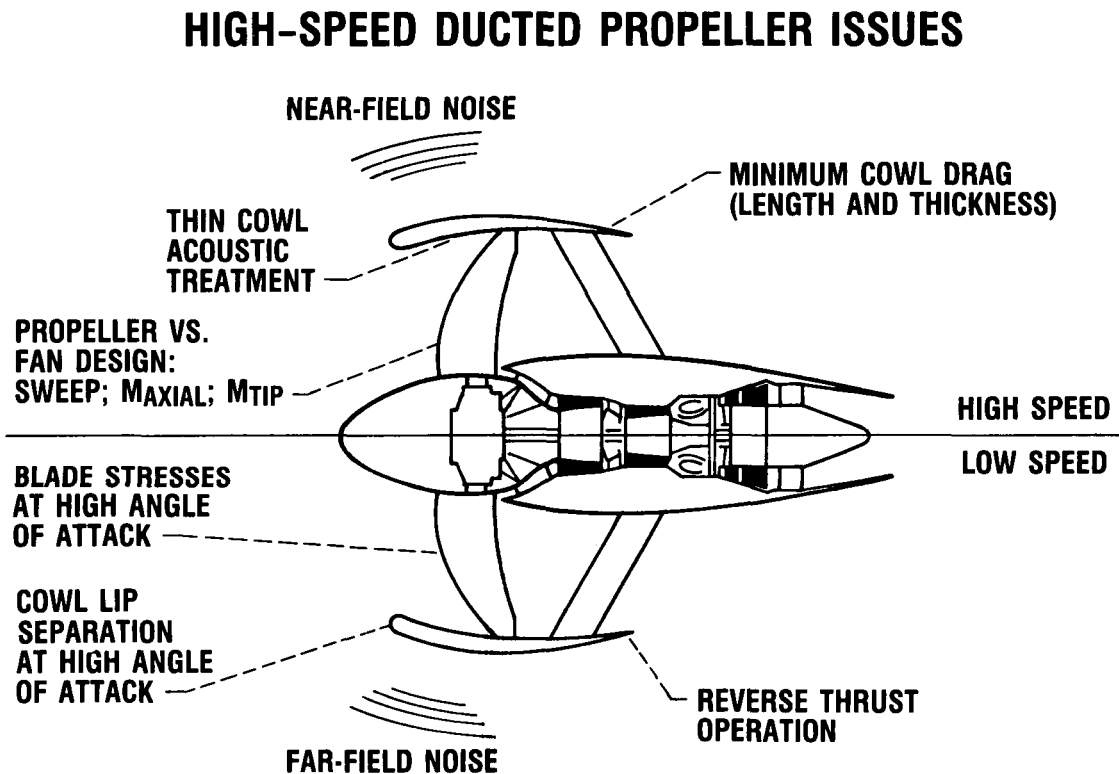
SWIRL RECOVERY VANE EXPERIMENT



CD-87-29507

HIGH-SPEED DUCTED PROPELLER ISSUES

Technical issues requiring research are noted for high-speed cruise in the upper half of the figure and for low-speed takeoff or approach in the lower half. At cruise, the drag of the large-diameter thin cowl must be minimized while achieving acceptable near-field sound levels. A synthesis of propeller and fan aerodynamic design methods is required to arrive at an optimum combination of sweep and of axial and tip Mach numbers. At low speed far-field community noise, cowl-lip separation at high angles of attack with the associated blade stresses and reverse thrust operation must each be addressed.



CD-87-29508

PROPELLER RESEARCH AREAS OF EMPHASIS

The status of current and future propeller research in each of the three disciplines (aerodynamics, acoustics, and aeroelasticity) is summarized. Presently, aerodynamic work emphasizes three-dimensional steady Euler solutions and performance measurements with some diagnostics, while future work is moving toward three-dimensional unsteady Euler and Navier-Stokes codes with more emphasis on detailed flow field diagnostics. Acoustically, three-dimensional codes are used with detailed steady aerodynamic input and extensive cruise and takeoff signatures have been measured for both single and counterrotation. Future efforts will emphasize unsteady aerodynamic inputs to the codes to describe interaction and installation effects and experiments will concentrate on detailed noise maps for installed configurations. Current aeroelastics focus has been in prediction and measurement of flutter boundaries and constructing the first generation of structural design optimization codes. Future emphasis in all three disciplines will involve addressing the technical issues associated with ultra high-bypass ducted propellers.

PROPELLER RESEARCH AREAS OF EMPHASIS

	PRESENT	FUTURE
AERODYNAMICS	<ul style="list-style-type: none">• 3D STEADY EULER CODES• PERFORMANCE MEASUREMENT, PROBE SURVEYS, & BLADE PRESSURES	<ul style="list-style-type: none">• 3D UNSTEADY EULER & NAVIER-STOKES CODES• DETAILED FLOW FIELD DIAGNOSTICS - LASER VELOCIMETER• ULTRA-HIGH BYPASS DUCTED PROPELLER PERFORMANCE
ACOUSTICS	<ul style="list-style-type: none">• 3D CODES USING DETAILED STEADY AERO INPUT• CRUISE AND TAKEOFF SIGNATURES FOR SRP & CRP INSTALLATIONS	<ul style="list-style-type: none">• INTERACTION & INSTALLATION EFFECTS FROM DETAILED UNSTEADY AERO INPUT• DETAILED NOISE MAPS FOR INSTALLED CONFIGURATIONS• CODES & DATA FOR SHORT, THIN DUCTS
AEROELASTICS	<ul style="list-style-type: none">• FLUTTER BOUNDARY MEASUREMENT & PREDICTION FOR SRP'S• FIRST GENERATION STRUCTURAL OPTIMIZATION CODES	<ul style="list-style-type: none">• FLUTTER BOUNDARY MEASUREMENT & PREDICTION FOR CRP'S• STALL FLUTTER & FORCED RESPONSE FOR SRP'S & CRP'S

CD-87-29509